Published in final edited form as:
Cell Rep. 2018 May 15; 23(7): 1948–1961. doi:10.1016/j.celrep.2018.04.055.

Loss of ABHD15 Impairs the Anti-lipolytic Action of Insulin by Altering PDE3B Stability and Contributes to Insulin Resistance

Wenmin Xia[#1], **Ariane R. Pessentheiner**[#1,10], **Dina C. Hofer**[1], **Melina Amor**[1], **Renate Schreiber**[2], **Gabriele Schoiswohl**[2], **Thomas O. Eichmann**[2,3], **Evelyn Walenta**[1], **Bianca Itariu**[4], **Gerhard Prager**[5], **Hubert Hackl**[6], **Thomas Stulnig**[4], **Dagmar Kratky**[7,8], **Thomas Rülicke**[9], and **Juliane G. Bogner-Strauss**[1,8,12,*]

[1]Institute of Biochemistry, Graz University of Technology, 8010 Graz, Austria

[2]Institute of Molecular Biosciences, University of Graz, 8010 Graz, Austria

[3]Center for Explorative Lipidomics, BioTechMed-Graz, 8010 Graz, Austria

[4]Christian Doppler Laboratory for Cardio-Metabolic Immunotherapy and Clinical Division of Endocrinology and Metabolism, Department of Medicine III, Medical University of Vienna, 1090 Vienna, Austria

[5]Department of Surgery, Medical University of Vienna, 1090 Vienna, Austria

[6]Biocenter, Division of Bioinformatics, Medical University of Innsbruck, 6020 Innsbruck, Austria

[7]Gottfried Schatz Research Center, Molecular Biology and Biochemistry, Medical University of Graz, 8010 Graz, Austria

[8]BioTechMed-Graz, 8010 Graz, Austria

[9]Institute of Laboratory Animal Science, University of Veterinary Medicine Vienna, 1210 Vienna, Austria

[10]Department of Medicine, University of California, San Diego, La Jolla, CA, USA

[#] These authors contributed equally to this work.

Summary

Elevated circulating fatty acids (FAs) contribute to obesity-associated metabolic complications, but the mechanisms by which insulin suppresses lipolysis are poorly understood. We show that α/β-

[*]Correspondence: juliane.bogner-strauss@tugraz.at.
[12]Lead Contact

Author Contributions

W.X. and A.R.P. performed animal experiments with Abhd15-KO mice. W.X. performed animal experiments with AdipoQ-Abhd15-KO mice. D.C.H. performed glucose incorporation assays. M.A. analyzed human microarray data and performed GEO submission. M.A., B.I., T.S., and G.P. obtained and analyzed data from the human cohort. R.S., G.S., and D.C.H. performed glucose uptake experiments in mice, *ex vivo* lipolysis assays, and re-esterification experiments. D.K. interpreted results. T.O.E. performed lipid analysis using ultra performance liquid chromatography-triple quadruple (UPLC-TQ). H.H. performed microarray data analysis. E.W., A.R.P., and T.R. generated Abhd15-KO and Abhd15-flox mouse lines. W.X. and A.R.P. analyzed data, and W.X. created the figures. J.G.B.-S. designed research, interpreted results, and wrote the manuscript with the help of A.R.P. and W.X.

Declaration of Interests

The authors declare no competing interests.

Europe PMC Funders Author Manuscripts

hydrolase domain-containing 15 (ABHD15) is required for the anti-lipolytic action of insulin in white adipose tissue (WAT). Neither insulin nor glucose treatments can suppress FA mobilization in global and conditional Abhd15-knockout (KO) mice. Accordingly, insulin signaling is impaired in Abhd15-KO adipocytes, as indicated by reduced AKT phosphorylation, glucose uptake, and *de novo* lipogenesis. *In vitro* data reveal that ABHD15 associates with and stabilizes phosphodiesterase 3B (PDE3B). Accordingly, PDE3B expression is decreased in the WAT of Abhd15-KO mice, mechanistically explaining increased protein kinase A (PKA) activity, hormone-sensitive lipase (HSL) phosphorylation, and undiminished FA release upon insulin signaling. Ultimately, Abhd15-KO mice develop insulin resistance. Notably, *ABHD15* expression is decreased in humans with obesity and diabetes compared to humans with obesity and normal glucose tolerance, identifying ABHD15 as a potential therapeutic target to mitigate insulin resistance.

Introduction

Adipose tissue (AT) is a multi-functional organ that plays an important role in lipid and glucose homeostasis for whole-body energy metabolism. Dysfunction of energy metabolism in AT leads to insulin resistance and contributes to the development of obesity and type 2 diabetes (T2D) (Rosen and Spiegelman, 2014). In mammals, AT is the predominant organ that serves as energy store in the form of triglycerides (TGs) in lipid droplets (LDs). Upon energy demand, these TGs are rapidly hydrolyzed by lipases (a process known as lipolysis), and the resulting fatty acids (FAs) released from LDs are used as an energy source in other organs (Guilherme et al., 2008). After food intake, glucose levels increase and activate insulin secretion from pancreatic islets; a rise of postprandial insulin inhibits AT lipolysis and promotes glucose uptake for *de novo* lipogenesis. Elevated plasma FA levels, also as a consequence of inappropriately controlled lipolysis, contribute to the development of insulin resistance and T2D (Armani et al., 2010; Gandotra et al., 2011a, 2011b; Girousse et al., 2013; Morigny et al., 2016; Savage et al., 2007). Understanding the detailed mechanisms by which insulin suppresses adipocyte lipolysis is critical to develop potential therapeutic strategies to mitigate insulin resistance and T2D.

In this study, we explored the physiological function of α/β-hydrolase domain-containing 15 (ABHD15) in lipid and glucose metabolism *in vivo* using global and AT-specific knockout (KO) mouse models. ABHD15 belongs to the α/β-hydrolase superfamily. This family consists of various lipases, esterases, and proteases that share an α/β fold as a common structural feature (Lord et al., 2013). Typically, ABHD proteins possess a catalytic triad consisting of a nucleophile (Ser, Cys, or Asp), an acid (aspartate or glutamate), and a conserved histidine residue enabling hydrolase activity. ABHD15 does not contain a nucleophile; therefore, a hydrolytic function is unlikely. ABHD15 also lacks another feature of ABHD proteins, namely, a Ser-X4-Asp motif, making a prediction of its enzymatic function difficult.

While the function of many family members, such as ABHD5 (CGI-58) (Lass et al., 2006) or ABHD6 (Thomas et al., 2013), is well described, the function of ABHD15 remains elusive. One previous study showed that a 47-kDa protein, most likely ABHD15 but its

Europe PMC Funders Author Manuscripts

identity was not clarified, is phosphorylated in 3T3-L1 adipocytes by protein kinase B (PKB/AKT) (Gridley et al., 2005), which is a major mediator of insulin signaling in AT. The same group proposed that this protein interacts with phosphodiesterase 3B (PDE3B) and regulates PDE3B protein amount in insulin-stimulated murine 3T3-L1 adipocytes (Chavez et al., 2006). PDE3B represents the major PDE3 isoform in adipocytes and is required for insulin to inhibit lipolysis by hydrolyzing cyclic AMP (cAMP) (Choi et al., 2006; DiPilato et al., 2015). Reduced cAMP levels lead to reduced phosphorylation and inactivation of hormone-sensitive lipase (HSL), which subsequently decreases lipolytic activity (Holm, 2003; Knighton et al., 1991; Watt et al., 2006).

Our previous work showed that *Abhd15* is highly expressed in ATs. Further, *Abhd15* expression was decreased in white AT (WAT) of aged and obese mice and in differentiated 3T3-L1 cells upon lipolytic stimulation (Walenta et al., 2013). The almost exclusive expression of *Abhd15* in AT (Walenta et al., 2013), its regulation by aging and FA concentrations, and its proposed interaction with PDE3B suggest that ABHD15 protein plays a critical role in insulin-regulated lipolysis. Herein we show that the expression of ABHD15 is regulated by the nutritional state and that ABHD15 is required for insulin-mediated suppression of lipolysis. Mechanistically, ABHD15 associates with and stabilizes PDE3B and, thereby, regulates its expression, leading to increased protein kinase A (PKA) activity, subsequent HSL phosphorylation, and increased lipolysis. Additionally, insulin signaling is impaired, ultimately leading to insulin resistance in Abhd15-KO mice. Of note, *ABHD15* expression is decreased in women with obesity and diabetes in comparison to women with obesity and normal glucose tolerance (GEO: GSE16415). These findings demonstrate that ABHD15 is essential for insulin-mediated suppression of lipolysis and is a crucial factor for the development of insulin resistance.

Results

Loss of Abhd15 Impacts Lipid- and FA-Related Pathways in AT

In line with previously reported *Abhd15* mRNA expression (Lord et al., 2013; Walenta et al., 2013), ABHD15 protein was mainly expressed in 3T3-L1 adipocytes and adipose depots, followed by a weak expression in liver and pancreas (Figures S1A and S1B). ABHD15 was not detected in skeletal muscle (SM) and cardiac muscle (CM) (Figure S1A). In WAT, ABHD15 was only expressed in mature adipocytes and primary adipocytes differentiated from stromal vascular cells (SVCs), but not in undifferentiated SVCs, suggesting that ABHD15 is not expressed in macrophages (Figure S1C).

To elucidate the physiological role of ABHD15 *in vivo*, we generated Abhd15-KO mice, as described in detail in the Experimental Procedures and depicted schematically in Figure 1A. The deletion of *Abhd15* exon 2 was confirmed by PCR (Figure 1B). Furthermore, successful deletion of ABHD15 protein was confirmed by immunoblotting in epididymal WAT (eWAT), subcutaneous WAT (sWAT), brown AT (BAT), liver, and pancreas (Figure 1C). Newborn Abhd15-KO pups exhibited no obvious defects and adult mutants of both sexes were fertile.

Europe PMC Funders Author Manuscripts

We hypothesized that ABHD15 plays a causal role in the development of insulin resistance. Both high-fat diet (HFD) and highglucose diet (HGD) have been shown to contribute to the development of insulin resistance (Oakes et al., 1997; Oka et al., 1980; Sun et al., 1977). Thus, we fed mice an HFD, an HGD, or a standard rodent chow diet until experiments were performed. Although silencing of Abhd15 reduced adipogenic differentiation of 3T3-L1 cells *in vitro* (Walenta et al., 2013), Abhd15-KO mice did not show differences in body weight and body mass composition on chow (Figures S1D and S1E), HGD (Figures S1F and S1G), and HFD (Figures S1H and S1I) when fed *ad libitum*. Plasma TG, FA, and glucose levels were measured in the fasted and in the refed state on all diets (Table S1). On chow and HFD, plasma parameters were unchanged between Abhd15-KO and wild-type (WT) mice except for increased TG concentrations in the refed state. On HGD, Abhd15-KO mice showed increased glucose levels in the refed state, while TG and FA levels were comparable to WT mice (Table S1). Food intake, energy expenditure, and respiratory exchange ratio (RER) were also similar in WT and Abhd15-KO mice on chow, HGD, and HFD fed *ad libitum* (Figures S1J–S1R).

To narrow down possible pathways that might be affected by the deletion of Abhd15, we performed transcriptome analysis of eWAT from chow diet-fed WT and Abhd15-KO mice, which were fasted overnight and then refed for 1 hr (GEO: GSE98321). The data revealed that 241 genes were more than 1.5-fold differentially expressed in the eWAT of Abhd15-KO compared to WT mice ($p < 0.01$) (Figure 1D) and 90 genes thereof with a false discovery rate (FDR) < 0.1. Among these dysregulated genes, 81 were upregulated and 160 downregulated in Abhd15-KO eWAT. Gene ontology/pathway analysis revealed that lipid metabolism-associated pathways were the most significantly downregulated processes in Abhd15-KO compared to WT mice (Figure 1E). Notably, mRNA expression of *Pde3b*, which was previously suggested to associate with ABHD15 in 3T3-L1 adipocytes (Chavez et al., 2006; Gridley et al., 2006), was strongly decreased in eWAT (Figure 1F). mRNA expression of *Pde3a*, a highly homologous subfamily member, was unchanged (Figure 1F), suggesting no compensatory upregulation in Abhd15-KO mice.

ABHD15 Associates with PDE3B and Regulates Its Stability and Expression

In accordance with mRNA expression, loss of ABHD15 markedly reduced PDE3B protein expression in eWAT (Figures 2A and 2B) and fully differentiated SVCs of Abhd15-KO mice when compared to controls (Figures 2C and 2D). Partial loss of ABHD15 in heterozygous Abhd15-KO mice (Figures 2A and 2B) and in differentiated 3T3-L1 cells that were transiently Abhd15 silenced (Figures S2A–S2C) was not sufficient to reduce PDE3B levels. Notably, re-expression of Abhd15 in Abhd15-KO SVCs *in vitro* was able to rescue PDE3B expression by around 50% (Figures 2E and 2F). Chavez and co-workers (Chavez et al., 2006) suggested that uncomplexed PDE3B undergoes degradation faster than PDE3B complexed with ABHD15. To directly test the stabilizing effect of ABHD15, we analyzed PDE3B protein stability by treating Pde3b-overexpressing COS7 cells with cycloheximide (CHX), which resulted in PDE3B degradation within less than 2 hr (Figure 2G, left blot). Remarkably, co-expression of Abhd15 prevented its degradation and stabilized PDE3B protein throughout the treatment (Figure 2G, right blot).

Although interaction of ABHD15 with PDE3B was proposed, the identity of ABHD15 as a complex partner was not directly confirmed (Chavez et al., 2006). We used a specific antibody for ABHD15, and we showed co-immunoprecipitation of ABHD15 with PDE3B in different cells, including Bnlcl2 hepatocytes (Figure S2D), COS7 cells (Figure 2H), and 3T3-L1 adipocytes (Figure 2I). The complexation of ABHD15 with PDE3B in 3T3-L1 cells was not affected by isoproterenol or insulin treatment (Figure 2I). This finding is in line with published data where insulin had no impact on the co-immunoprecipitation of ABHD15 and PDE3B (Chavez et al., 2006). Western blotting experiments revealed that ABHD15, like PDE3B, is a membrane-associated protein (Figure S2E), making an interaction of these proteins even more likely.

Interestingly, silencing of PDE3B in fully differentiated 3T3-L1 cells also reduced the expression of ABHD15 (Figures S2H–S2J), indicating that ABHD15 and PDE3B regulate each other's protein expression and/or stability presumably via complex formation.

Disruption of Insulin-Mediated Suppression of FA Release in Abhd15-KO Mice

PDE3B has been shown to be required for insulin-mediated suppression of lipolysis via the cAMP-dependent protein kinase pathway (Choi et al., 2006; DiPilato et al., 2015). In AT, lipolysis is activated by fasting and abrogated by refeeding, which depends on the potent anti-lipolytic actions of insulin (Duncan et al., 2007). Interestingly, ABHD15 expression in eWAT was reduced after overnight fasting, while it was increased upon 1 and 2 hr of refeeding (Figures 3A and 3B). To investigate whether Abhd15 itself regulates lipolysis, we performed *in vitro* analyses in 3T3-L1 cells. Overexpression of ABHD15 per se had no influence on basal or insulin-suppressed free fatty acid (FFA) and glycerol release (Figures S2L and S2M) and phosphorylation of HSL or PKA substrates (Figure S2K), neither in the presence nor upon silencing of PDE3B (Figures S2K–S2M).

To assess the impact of Abhd15 deletion on insulin-mediated suppression of lipolysis *in vivo*, we fasted mice overnight, administered insulin, and determined its anti-lipolytic effect by measuring plasma FA levels. For *ad libitum* chow diet-fed mice, plasma FAs were similar in WT and Abhd15-KO mice, and overnight fasting activated FA release in both genotypes to the same extent (Figure 3C). Importantly, insulin injection strongly reduced plasma FA in WT mice, while circulating FA concentrations in Abhd15-KO mice remained as high as in the fasted state (Figures 3C and S3A–S3C). Similarly, a glucose gavage approach, to mimic a more physiological condition to stimulate endogenous insulin secretion, also resulted in unsuppressed FA release in Abhd15-KO mice (Figure 3D). These data indicate unsuppressed lipolysis in WAT. Accordingly, the canonical pathway that regulates insulin-suppressed lipolysis downstream of PDE3B is altered in Abhd15-KO mice. While cAMP levels showed only trends to be elevated in Abhd15-KO mice (Figure S3D), phosphorylation of PKA substrates was increased in eWAT and sWAT of Abhd15-KO mice after overnight fasting (saline) and insulin stimulation (Figures 3E and S3E). Accordingly, phosphorylation of HSL at S660, one of three HSL phosphorylation sites that control HSL activity (Anthonsen et al., 1998), was markedly increased in Abhd15-KO mice when compared to WT mice (Figures 3F, 3G, S3F, and S3G).

Next, we measured lipolysis in fat pads *ex vivo* derived from WT and Abhd15-KO mice to directly assess the impact of ABHD15 on lipolysis. As expected, FA release from WT fat pads was lower upon insulin than during basal conditions (Figure 3H). Again, no insulin-mediated reduction in FA release was observed in Abhd15-KO fat pads (Figure 3H). In the presence of small molecule inhibitors for adipose TG lipase (ATGL) and HSL (iATGL and iHSL, respectively), however, FA release from Abhd15-KO fat pads was decreased, but it was still higher than from WT fat pads (Figure 3H). Glycerol release from *ex vivo* fat pads was comparable between WT and Abhd15-KO mice in the absence and presence of ATGL or HSL inhibitors (Figure S3H).

In addition to increased lipolysis, reduced FA re-esterification might explain elevated plasma FA concentrations in Abhd15-KO mice upon insulin signaling. qRT-PCR results supported a reduced re-esterification potential, because mRNA expression of genes involved in lipogenesis (*Srebp1c*, *Scd1*, *Acsl1*, *Dgat1*, and *Pepck*) was reduced in the fasted state (Figure S3I), when re-esterification potential in adipocytes is highest (Chitraju et al., 2017). However, in the refed state in which ABHD15 may play a key role in insulin-mediated suppression of lipolysis, expression levels of the above-mentioned genes were unchanged in Abhd15-KO mice, except for *Scd1* (Figure S3I). To assess whether ABHD15 has a cell-autonomous effect on FA re-esterification, we tested the incorporation of radiolabeled oleic acid into TG in differentiated primary Abhd15-KO and WT adipocytes upon lipolytic stimulation. However, we did not observe any differences between genotypes (Figure S3J), arguing against reduced re-esterification. Our data rather suggest that impaired suppression of insulin-mediated lipolysis is causative for increased plasma FA in Abhd15-KO mice.

When lipolysis is activated, WAT is the main organ to release FAs to the circulation. Thus, in line with increased FA release from Abhd15-KO AT, sWAT weight was smaller in Abhd15-KO than in WT mice after insulin injection, while no changes were observed in fasted and fed states (Figure 3I). Additionally, BAT weight was reduced in fasted and insulin-injected states, while we found no changes in eWAT and liver weights in Abhd15-KO compared to WT mice (Figure 3I). Consistent with reduced AT weight, H&E staining of sWAT showed a profound reduction in adipocyte size in Abhd15-KO mice compared to WT mice 20 min after insulin administration (Figures 3J and 3K). These data strongly suggest that ABHD15 plays a role in insulin-mediated suppression of lipolysis.

Abhd15-KO Mice Show Impaired Insulin-Dependent Glucose Metabolism and Develop Insulin Resistance

Increased plasma FA concentrations have been discussed as a deleterious factor in the development of insulin resistance (Perry et al., 2015; Samuel and Shulman, 2012). Therefore, we assessed whether impaired insulin-mediated suppression of lipolysis upon loss of ABHD15 affects glucose metabolism. We observed a moderately higher plasma insulin concentration (62%, $p = 0.068$) in Abhd15-KO mice after a single glucose bolus (Figure 4A). Yet, these increased insulin levels did not suppress plasma FA levels in Abhd15-KO mice when compared to WT mice (Figure 3D). Insulin inhibits lipolysis, but it also stimulates glucose uptake by activating glucose transporter type 4 (GLUT4) translocation to the plasma membrane. Thus, we investigated glucose uptake into tissues of

WT and Abhd15-KO mice after gavage of ^{3}H-deoxyglucose that cannot be metabolized after uptake. As shown in Figure 4B, glucose uptake into eWAT, heart, and liver was decreased in Abhd15-KO mice compared to WT mice, while there were no differences in sWAT, SM, and BAT.

In adipocytes, glucose is used for *de novo* lipogenesis (DNL) upon insulin stimulation to store energy in the form of TG in LDs. To investigate DNL, we isolated SVCs from sWAT of Abhd15-KO and WT mice and differentiated them into adipocytes. SVCs from both genotypes differentiated to the same extent, as evidenced by unchanged C/EBPα protein expression and oil red O staining (Figures S4A and S4B). Under basal conditions, fully differentiated WT and Abhd15-KO SVCs incorporated the same amount of glucose into total lipids (Figure 4C). Insulin strongly stimulated DNL in both genotypes, but Abhd15-KO adipocytes incorporated significantly less glucose into neutral lipids than WT adipocytes (Figure 4C). In particular, we observed reduced glucose incorporation into FFA, monoacylglycerol (MAG), and diacylglycerol (DAG) (Figure 4C), respectively, while there was no difference in TGs and cholesteryl esters (CEs) (Figure S4C). Supporting these data, qRT-PCR analysis showed that glucose metabolism (glucose kinase) and DNL pathway genes, such as *Fas* and *AceCS*, were reduced in Abhd15-KO mice in the refed state (Figure S3I).

PKB/AKT is known as a master regulator of glucose and lipid metabolism in adipocytes (Kohn et al., 1996; Saltiel and Kahn, 2001). Phosphorylation of PKB/AKT was strongly decreased in eWAT and sWAT of Abhd15-KO mice when compared to controls (Figures 4D, 4E, S4D, and S4E). Additionally, adiponectin levels were markedly reduced in Abhd15-KO compared to WT mice independent of age (Figures 4F and 4G). Decreased adiponectin levels are considered an early indicator of insulin resistance (Cnop et al., 2003; Kadowaki et al., 2006). Upon aging, insulin sensitivity decreases, which correlates with lower adiponectin levels (Hotta et al., 2001). Indeed, young Abhd15-KO mice showed moderately reduced insulin sensitivity with no changes in glucose tolerance (Figures S4F and S4G), while old Abhd15-KO mice (≥60 weeks of age) showed impaired insulin sensitivity and glucose tolerance when compared to WT mice (Figures 4H and 4I). Supporting our data, bioinformatic analysis of published microarray data (GEO: GSE16415) from human omental AT (OWAT) revealed that *ABHD15* expression was 2-fold lower in women with obesity and diabetes (BMI > 30 kg/m^2, age > 55 years) compared to age-matched women with obesity and normal glucose tolerance (Table S2). Except for *PDE3B* and the ATGL coactivator *ABHD5* (*CGI58*), several other PDE and ABHD family members showed no deregulation in this cohort (Table S2).

To validate these data, we measured *ABHD15* gene expression in OWAT from 11 patients with severe obesity by qPCR. Subsequently, the data were correlated with several metabolic parameters obtained from the cohort by Spearman's rank. We observed that *ABHD15* expression in OWAT positively correlated with insulin sensitivity estimators, such as oral glucose insulin sensitivity (OGIS), insulin sensitivity index (ISI), and clamp-like index (CLIX), and negatively correlated with insulin resistance estimators, including first and second phase response to a glucose challenge and the area under the curve for insulin during

Europe PMC Funders Author Manuscripts

the oral glucose tolerance test (OGTT). Furthermore, *ABHD15* mRNA levels in OWAT negatively correlated with interleukin-6 (IL-6) and FFA levels in serum (Table 1).

Together, these data demonstrate that ABHD15 ablation impairs insulin signaling, most probably via PDE3B, and subsequently leads to insulin resistance.

Abhd15-KO Mice Develop Insulin Resistance When Fed High-Glucose and High-Fat Diets

In Abhd15-KO mice, the disrupted anti-lipolytic effect of insulin was also evident from elevated plasma FA levels upon HGD (Figure 5A) and HFD feeding (Figure 5B), supporting the role of ABHD15 as a regulator of insulin-suppressed lipolysis. In fat pads from HFD-fed Abhd15-KO mice, basal FA release was increased, which could not be diminished by insulin addition (Figure 5C). Although the insulin-mediated suppression of lipolysis was consistently abrogated in Abhd15-KO mice fed HGD and HFD (Figures 5A and 5B), they did not suffer from reduced insulin sensitivity after 12 weeks on the respective diet (Figures S4H and S4J). At this point, glucose tolerance was also unchanged upon HGD feeding (Figure S4I), but it was already impaired in HFD-fed Abhd15-KO mice (Figure S4K). After HGD feeding for ≥18 weeks, Abhd15-KO mice had lower adiponectin levels and higher postprandial insulin and glucose levels, despite unchanged food intake during refeeding and leptin levels (Figures 5D–5H). Accordingly, insulin sensitivity was reduced (Figure 5I). In addition, long-term feeding of HFD (30 weeks) evoked a strongly impaired glucose tolerance in Abhd15-KO mice (Figure 5J). However, WT and Abhd15-KO mice were insulin resistant at this point, and differences between the genotypes were no longer observed (Figure 5K). These data confirm that ABHD15 ablation leads to insulin resistance independently of the diet consumed.

AT-Specific Ablation of ABHD15 Is Responsible for the Phenotype Observed in Global Abhd15-KO Mice

Finally, we aimed to investigate whether the phenotype of total Abhd15-KO mice is exclusively due to *Abhd15* deletion in AT. Therefore, we used adiponectin (AdipoQ)-driven Cre transgenic mice to delete *Abhd15* specifically in WAT and BAT (AdipoQ-Abhd15-KO; Figure 6A). In fasted AdipoQ-Abhd15-KO mice, injection of insulin or glucose gavage also failed to inhibit FA release on chow and HGD (Figures S5A and 6B). Chow dietfed AdipoQ-Abhd15-KO mice also showed reduced fat mass in the fasted and fed states (Figure S5B), while plasma and metabolic parameters were unaltered (Figures S5C–S5F). In HGD-fed AdipoQ-Abhd15-KO mice, body weight, body mass composition, energy expenditure, and plasma insulin levels were unchanged (Figures S5G–S5J). Similar to Abhd15-KO mice, HGD diet-fed AdipoQ-Abhd15-KO mice had strongly decreased expression of genes involved in lipid metabolism (Figures 6C and S5K), reduced PDE3B protein expression (Figures S5L and S5M), and lower plasma adiponectin concentrations (Figure 6D). Accordingly, glucose tolerance and insulin sensitivity (Figures 6E and 6F) were markedly diminished. The significantly lower RER suggests that AdipoQ-Abhd15-KO mice on HGD preferentially oxidize lipids during the dark phase and in the refed state when compared to controls (Figure 6G). These results strongly suggest an exclusive role of ABHD15 for insulin-mediated suppression of lipolysis in WAT, thereby influencing whole-body lipid and glucose metabolism.

Europe PMC Funders Author Manuscripts

Discussion

Dynamic metabolic transition from the fasting to the fed or postprandial state and vice versa is of great importance for maintaining energy homeostasis *in vivo*. In this study, we present ABHD15 as a crucial player in regulating insulin-mediated suppression of lipolysis and the development of insulin resistance. ABHD15 is highly expressed in ATs, the main organs where lipolysis occurs. We have previously shown that *Abhd15* mRNA expression in the WAT is decreased in fasted mice and in genetically obese mice with T2D (Walenta et al., 2013). In the present study, we demonstrate that ABHD15 protein expression is reduced by fasting and induced by refeeding in the WAT of lean and healthy mice. Moreover, *ABHD15* expression is diminished in the WAT of patients with obesity and diabetes when compared to patients with obesity and normal glucose tolerance. In addition, we showed that ABHD15 mRNA expression negatively correlated with markers of insulin resistance in humans. However, the rather small sample size can be taken as a limitation of this analysis.

In all conditions associated with reduced ABHD15 expression, plasma FA levels are elevated. Plasma FA concentrations are tightly controlled by lipolysis, a process turned on by fasting to provide FAs as an energy source for peripheral tissues while turned off upon (re)feeding by insulin signaling. Elevated circulating FA levels contribute to insulin resistance in both animals and humans (Boden, 1997; Gandotra et al., 2011a, 2011b; Kelley et al., 1993; Savage et al., 2007). Recently, it has been reported that the failure of insulin to decrease the supply of FAs as substrate for liver gluconeogenesis leads to systemic insulin resistance (Perry et al., 2015). Although many aspects have been clarified, the detailed molecular mechanisms of how insulin suppresses lipolysis in adipocytes is still elusive. Since it became increasingly evident that elevated plasma FA levels lead to ectopic lipid deposition and insulin resistance, the search for regulators of insulin-mediated inhibition of lipolysis might pave the way for therapeutic applications. We therefore used constitutive and AT-specific Abhd15-KO mice to test our hypothesis that ABHD15 is an important player in insulin-mediated suppression of lipolysis and the development of insulin resistance.

Loss of ABHD15 resulted in a failure of insulin to decrease plasma FA levels at both experimental (insulin-injected) and physiological conditions independent of diet and age. However, plasma glycerol concentrations were unchanged in these mice (data not shown). The underlying reason(s) for this discrepancy between reduced FA but normal glycerol levels is currently unknown but will be important to address in future studies. We hypothesize that elevated FA concentrations upon *Abhd15* deletion are at least partially due to the simultaneous reduction of PDE3B in WAT, as the unsuppressed lipolysis phenotype of our Abhd15-KO mouse models was also described in Pde3b-null mice (Choi et al., 2006). Consistently, it has been previously suggested that ABHD15 binds to PDE3B and regulates its expression in 3T3-L1 adipocytes (Chavez et al., 2006). However, this former study used an antibody generated with a peptide directed against 15 amino acids (aa) at the C terminus of ABHD15 that also shows homology with ABHD1 and ABHD3. We used an antibody directed against the whole protein sequence, and we confirmed in various cell lines that ABHD15 co-immunoprecipitates with PDE3B. Within this complex, ABHD15 likely regulates PDE3B expression and/or protein stability, as its expression is also impaired in the WAT of Abhd15-KO mice. A regulation of PDE3B by ABHD15 is also supported by the

fact that both proteins are expressed as membrane proteins. Importantly, we could rescue PDE3B expression by re-expressing ABHD15 in differentiating Abhd15-KO SVCs. Supporting our hypothesis, PDE3B protein stability is massively increased when ABHD15 is co-expressed. Vice versa, also PDE3B seems to influence ABHD15 stability, since ABHD15 protein expression is decreased in Pde3b-silenced 3T3-L1 cells.

Phosphorylation by AKT or PKA was shown to increase the activity of PDE3B (Kitamura et al., 1999; Perino et al., 2011). However, disrupted phosphorylation of PDE3B on both AKT and PKA phosphorylation sites did not interfere with insulin-mediated suppression of lipolysis (DiPilato et al., 2015). Therefore, we did not further investigate PDE3B phosphorylation in our mouse models, but we suggest that ABHD15 plays a crucial role in regulating the amount of PDE3B protein and downstream lipolysis. Decreased PDE3B protein/activity increases cAMP levels and activates PKA (Choi et al., 2006; DiPilato et al., 2015; Maurice et al., 2003). In line with this, we observed increased phosphorylation of PKA substrates and HSL in the WAT of Abhd15-KO mice after overnight fasting and in an insulin-injected state. Concomitantly, FA release into the bloodstream is not suppressed by insulin in Abhd15-KO mice. Fat pads isolated from Abhd15-KO animals showed the same unsuppressed FA release *ex vivo*, which could be reduced by ATGL and HSL inhibitors. Thus, unsuppressed lipolysis is supposed to be, at least in part, the cause of this phenotype.

In adipocytes, activated/phosphorylated PDE3B has also been shown to form large macro-molecular complexes, so-called signalosomes, with insulin receptor substrate (IRS), phosphoinositide 3-kinase (PI3K), AKT, caveolin-1, and protein phosphatase 2 (PP2A) (Ahmad et al., 2007, 2012; Kitamura et al., 1999; Rondinone et al., 2000). It is, however, unlikely that the reduced amount of PDE3B in Abhd15-KO mice regarding signalosome formation affects the insulin signaling pathway, as Pde3b-KO adipocytes show neither reduced AKT phosphorylation nor reduced glucose uptake (Choi et al., 2006; DiPilato et al., 2015). Nevertheless, reduced PDE3B protein might impact the formation of the signalosome and its localization to the LD and, therefore, it might impact insulin-suppressed lipolysis.

Decreased but also increased adipocyte lipolysis have been shown to improve insulin resistance (Ahmadian et al., 2009, 2010, 2011; Haemmerle et al., 2006; Samuel and Shulman, 2012; Schweiger et al., 2017). In humans with obesity, however, persistently elevated circulating FA concentrations can account for a large part of insulin resistance (Boden, 2011; Girousse et al., 2013; Liang et al., 2013). Unrestrained lipolysis in humans with mutations in perilipin 1 leads to severe insulin resistance (Gandotra et al., 2011a, 2011b), underlining a role of increased plasma FA concentrations in the pathogenesis of this disease. Pharmacological inhibition of ATGL or HSL also improves insulin sensitivity in genetically or diet-induced obesity (Girousse et al., 2013; Schweiger et al., 2017). Accordingly, Abhd15-KO mice might develop insulin resistance due to unsuppressed adipocyte FA release.

Glucose uptake and DNL in WAT are largely dependent on the insulin/AKT/GLUT4 pathway (Kohn et al., 1996). Interestingly, in the WAT of Abhd15-KO mice, phosphorylation of AKT is decreased upon insulin injection, and, thus, it might be responsible for the reduced glucose uptake and incorporation into *de novo* synthesized

lipids. In adipocytes, glucose uptake controls DNL, which plays a crucial role in whole-body insulin sensitivity (Herman et al., 2012; Roberts et al., 2009). Improved insulin sensitivity in HFD-fed heterozygous HSL-KO mice was associated with increased DNL (Girousse et al., 2013). Thus, it is also conceivable that the reduced DNL observed in our mouse models contributes to the development of insulin resistance. Furthermore, reduced adiponectin levels, an early indicator of insulin resistance (Cnop et al., 2003; Hotta et al., 2001), might add to the observed phenotype.

It has been suggested that PDE3B is involved in the secretion of adiponectin in adipocytes by an unknown mechanism (Cong et al., 2007). PDE3B is part of the signalosome that also contains PP2A. Very recently, Hatting et al. (2017) showed that PP2A inhibition increases cAMP response element-binding protein (CREB) phosphorylation. Phosphorylated CREB (pCREB) activates ATF3, and this transcription factor inhibits the expression of adiponectin and *Glut4*, thereby leading to insulin resistance (Qi et al., 2009). PDE3B is reduced in adipocytes from patients with diabetes (Engfeldt et al., 1982), and Pde3b-KO mice develop insulin resistance (Choi et al., 2006). These mice, however, have elevated adiponectin levels, and the insulin resistance was attributed to their hepatic and pancreatic phenotype (Choi et al., 2006). In contrary, our data reveal that the insulin resistance in Abhd15-KO mice is mainly due to the AT phenotype. Although Abhd15-KO mice only show an ~50% reduction in PDE3B expression, their WAT phenotype on the molecular level is much stronger than the one observed in Pde3b-KO mice. Underlining these observations, the AdipoQ-Abhd15-KO mouse phenocopies the global Abhd15-KO mouse, despite undiminished PDE3B expression in any other tissue than ATs. Thus, we hypothesize that ABHD15 has a function apart from the regulation of PDE3B that warrants future studies.

Together, our data demonstrate that ABHD15 is indispensable for insulin-mediated suppression of lipolysis and its ablation leads to insulin resistance in mice. These findings, together with the reduced *ABHD15* expression in humans with obesity and diabetes, identify ABHD15 as a potential therapeutic target for treating age- and obesity-associated insulin resistance.

Experimental Procedures

Animal Study

The study was approved by the institutional ethics committee, and experiments were performed according to the guidelines of the Austrian Federal Ministry of Science and Research. Experiment licenses were granted under BMWF-68.205/0258-II/3b/2011, BMWF-66.007/0026-WF/V/3b/2015, and BMWF-66.007/0008-WF/V/3b/2016. If not otherwise stated, age-matched male Abhd15-KO and WT mice, Abhd15-flox mice, and Abhd15-flox+/AdipoQ-cre mice (except for SVC isolation we used female, 10-week-old mice) were used for each experiment in this study (age and number of mice used are noted in the figure legends).

Human Study

The study was performed in accordance with the Helsinki Declaration of 1975 as revised in 1983 and with Good Clinical Practice guidelines, and it was approved by the Ethics Committee of the Medical University of Vienna and Göttlicher Heiland Hospital (EK Nr. 963/2009, EK Nr. 488/2006, and E10-N01-01). All subjects provided written informed consent.

Statistical Analysis

If not otherwise stated results are mean values ± SD of at least three independent experiments or results show one representative experiment out of at least three. Statistical significance was determined using the unpaired 2-tailed Student's t test or the two-way ANOVA test. For statistical analysis, GraphPad Prism software was used (§, #, *$p < 0.05$, **$p < 0.01$, and ***$p < 0.001$). Correlations of the human dataset in Table 1 were explored by Spearman's method. Statistical significance was set at $p < 0.05$. All statistical analyses were performed with IBM SPSS Statistics for Windows, version 21.0 (IBM, Armonk, NY).

Detailed methods are described in the Supplemental Experimental Procedures.

Supplementary Material

Refer to Web version on PubMed Central for supplementary material.

Acknowledgments

This work was funded by the Austrian Science Fund FWF (SFB LIPTOX F3018, P27108, P28882, and DK-MCD W1226). We acknowledge the support of NAWI Graz and the technical support of Thomas Schreiner, Wolfgang Krispel, Rita Lang, and Silvia Schauer. We want to thank Robert Zimmermann for providing the ATGL inhibitor and Wael Al-Zoughbi and Gerald Hoefler for helping with H&E microscopy.

References

Ahmad F, Lindh R, Tang Y, Weston M, Degerman E, Manganiello VC. Insulin-induced formation of macromolecular complexes involved in activation of cyclic nucleotide phosphodiesterase 3B (PDE3B) and its interaction with PKB. Biochem J. 2007; 404:257–268. [PubMed: 17324123]

Ahmad F, Degerman E, Manganiello VC. Cyclic nucleotide phosphodiesterase 3 signaling complexes. Horm Metab Res. 2012; 44:776–785. [PubMed: 22692928]

Ahmadian M, Duncan RE, Varady KA, Frasson D, Hellerstein MK, Birkenfeld AL, Samuel VT, Shulman GI, Wang Y, Kang C, Sul HS. Adipose overexpression of desnutrin promotes fatty acid use and attenuates diet-induced obesity. Diabetes. 2009; 58:855–866. [PubMed: 19136649]

Ahmadian M, Wang Y, Sul HS. Lipolysis in adipocytes. Int J Biochem Cell Biol. 2010; 42:555–559. [PubMed: 20025992]

Ahmadian M, Abbott MJ, Tang T, Hudak CS, Kim Y, Bruss M, Hellerstein MK, Lee HY, Samuel VT, Shulman GI, et al. Desnutrin/ATGL is regulated by AMPK and is required for a brown adipose phenotype. Cell Metab. 2011; 13:739–748. [PubMed: 21641555]

Anthonsen MW, Rönnstrand L, Wernstedt C, Degerman E, Holm C. Identification of novel phosphorylation sites in hormone-sensitive lipase that are phosphorylated in response to isoproterenol and govern activation properties in vitro. J Biol Chem. 1998; 273:215–221. [PubMed: 9417067]

Armani A, Mammi C, Marzolla V, Calanchini M, Antelmi A, Rosano GM, Fabbri A, Caprio M. Cellular models for understanding adipogenesis, adipose dysfunction, and obesity. J Cell Biochem. 2010; 110:564–572. [PubMed: 20512917]

Boden G. Role of fatty acids in the pathogenesis of insulin resistance and NIDDM. Diabetes. 1997; 46:3–10. [PubMed: 8971073]

Boden G. Obesity, insulin resistance and free fatty acids. Curr Opin Endocrinol Diabetes Obes. 2011; 18:139–143. [PubMed: 21297467]

Chavez JA, Gridley S, Sano H, Lane WS, Lienhard GE. The 47kDa Akt substrate associates with phosphodiesterase 3B and regulates its level in adipocytes. Biochem Biophys Res Commun. 2006; 342:1218–1222. [PubMed: 16516160]

Chitraju C, Mejhert N, Haas JT, Diaz-Ramirez LG, Grueter CA, Imbriglio JE, Pinto S, Koliwad SK, Walther TC, Farese RV Jr. Triglyceride Synthesis by DGAT1 Protects Adipocytes from Lipid-Induced ER Stress during Lipolysis. Cell Metab. 2017; 26:407–418.e3. [PubMed: 28768178]

Choi YH, Park S, Hockman S, Zmuda-Trzebiatowska E, Svennelid F, Haluzik M, Gavrilova O, Ahmad F, Pepin L, Napolitano M, et al. Alterations in regulation of energy homeostasis in cyclic nucleotide phospho-diesterase 3B-null mice. J Clin Invest. 2006; 116:3240–3251. [PubMed: 17143332]

Cnop M, Havel PJ, Utzschneider KM, Carr DB, Sinha MK, Boyko EJ, Retzlaff BM, Knopp RH, Brunzell JD, Kahn SE. Relationship of adiponectin to body fat distribution, insulin sensitivity and plasma lipoproteins: evidence for independent roles of age and sex. Diabetologia. 2003; 46:459–469. [PubMed: 12687327]

Cong L, Chen K, Li J, Gao P, Li Q, Mi S, Wu X, Zhao AZ. Regulation of adiponectin and leptin secretion and expression by insulin through a PI3K-PDE3B dependent mechanism in rat primary adipocytes. Biochem J. 2007; 403:519–525. [PubMed: 17286556]

DiPilato LM, Ahmad F, Harms M, Seale P, Manganiello V, Birnbaum MJ. The Role of PDE3B Phosphorylation in the Inhibition of Lipolysis by Insulin. Mol Cell Biol. 2015; 35:2752–2760. [PubMed: 26031333]

Duncan RE, Ahmadian M, Jaworski K, Sarkadi-Nagy E, Sul HS. Regulation of lipolysis in adipocytes. Annu Rev Nutr. 2007; 27:79–101. [PubMed: 17313320]

Engfeldt P, Arner P, Bolinder J, Ostman J. Phosphodiesterase activity in human subcutaneous adipose tissue in insulin- and noninsulin-dependent diabetes mellitus. J Clin Endocrinol Metab. 1982; 55:983–988. [PubMed: 6288760]

Gandotra S, Le Dour C, Bottomley W, Cervera P, Giral P, Reznik Y, Charpentier G, Auclair M, Delépine M, Barroso I, et al. Perilipin deficiency and autosomal dominant partial lipodystrophy. N Engl J Med. 2011a; 364:740–748. [PubMed: 21345103]

Gandotra S, Lim K, Girousse A, Saudek V, O'Rahilly S, Savage DB. Human frame shift mutations affecting the carboxyl terminus of perilipin increase lipolysis by failing to sequester the adipose triglyceride lipase (ATGL) coactivator AB-hydrolase-containing 5 (ABHD5). J Biol Chem. 2011b; 286:34998–35006. [PubMed: 21757733]

Girousse A, Tavernier G, Valle C, Moro C, Mejhert N, Dinel AL, Houssier M, Roussel B, Besse-Patin A, Combes M, et al. Partial inhibition of adipose tissue lipolysis improves glucose metabolism and insulin sensitivity without alteration of fat mass. PLoS Biol. 2013; 11:e1001485. [PubMed: 23431266]

Gridley S, Lane WS, Garner CW, Lienhard GE. Novel insulin-elicited phosphoproteins in adipocytes. Cell Signal. 2005; 17:59–66. [PubMed: 15451025]

Gridley S, Chavez JA, Lane WS, Lienhard GE. Adipocytes contain a novel complex similar to the tuberous sclerosis complex. Cell Signal. 2006; 18:1626–1632. [PubMed: 16490346]

Guilherme A, Virbasius JV, Puri V, Czech MP. Adipocyte dysfunctions linking obesity to insulin resistance and type 2 diabetes. Nat Rev Mol Cell Biol. 2008; 9:367–377. [PubMed: 18401346]

Haemmerle G, Lass A, Zimmermann R, Gorkiewicz G, Meyer C, Rozman J, Heldmaier G, Maier R, Theussl C, Eder S, et al. Defective lipolysis and altered energy metabolism in mice lacking adipose triglyceride lipase. Science. 2006; 312:734–737. [PubMed: 16675698]

Hatting M, Rines AK, Luo C, Tabata M, Sharabi K, Hall JA, Verdeguer F, Trautwein C, Puigserver P. Adipose Tissue CLK2 Promotes Energy Expenditure during High-Fat Diet Intermittent Fasting. Cell Metab. 2017; 25:428–437. [PubMed: 28089567]

Herman MA, Peroni OD, Villoria J, Schön MR, Abumrad NA, Blüher M, Klein S, Kahn BB. A novel ChREBP isoform in adipose tissue regulates systemic glucose metabolism. Nature. 2012; 484:333–338. [PubMed: 22466288]

Holm C. Molecular mechanisms regulating hormone-sensitive lipase and lipolysis. Biochem Soc Trans. 2003; 31:1120–1124. [PubMed: 14641008]

Hotta K, Funahashi T, Bodkin NL, Ortmeyer HK, Arita Y, Hansen BC, Matsuzawa Y. Circulating concentrations of the adipocyte protein adiponectin are decreased in parallel with reduced insulin sensitivity during the progression to type 2 diabetes in rhesus monkeys. Diabetes. 2001; 50:1126–1133. [PubMed: 11334417]

Kadowaki T, Yamauchi T, Kubota N, Hara K, Ueki K, Tobe K. Adiponectin and adiponectin receptors in insulin resistance, diabetes, and the metabolic syndrome. J Clin Invest. 2006; 116:1784–1792. [PubMed: 16823476]

Kelley DE, Mokan M, Simoneau J-A, Mandarino LJ. Interaction between glucose and free fatty acid metabolism in human skeletal muscle. J Clin Invest. 1993; 92:91–98. [PubMed: 8326021]

Kitamura T, Kitamura Y, Kuroda S, Hino Y, Ando M, Kotani K, Konishi H, Matsuzaki H, Kikkawa U, Ogawa W, Kasuga M. Insulin-induced phosphorylation and activation of cyclic nucleotide phosphodiesterase 3B by the serine-threonine kinase Akt. Mol Cell Biol. 1999; 19:6286–6296. [PubMed: 10454575]

Knighton DR, Zheng JH, Ten Eyck LF, Xuong NH, Taylor SS, Sowadski JM. Structure of a peptide inhibitor bound to the catalytic subunit of cyclic adenosine monophosphate-dependent protein kinase. Science. 1991; 253:414–420. [PubMed: 1862343]

Kohn AD, Summers SA, Birnbaum MJ, Roth RA. Expression of a constitutively active Akt Ser/Thr kinase in 3T3-L1 adipocytes stimulates glucose uptake and glucose transporter 4 translocation. J Biol Chem. 1996; 271:31372–31378. [PubMed: 8940145]

Lass A, Zimmermann R, Haemmerle G, Riederer M, Schoiswohl G, Schweiger M, Kienesberger P, Strauss JG, Gorkiewicz G, Zechner R. Adipose triglyceride lipase-mediated lipolysis of cellular fat stores is activated by CGI-58 and defective in Chanarin-Dorfman Syndrome. Cell Metab. 2006; 3:309–319. [PubMed: 16679289]

Liang H, Tantiwong P, Sriwijitkamol A, Shanmugasundaram K, Mohan S, Espinoza S, Defronzo RA, Dubé JJ, Musi N. Effect of a sustained reduction in plasma free fatty acid concentration on insulin signalling and inflammation in skeletal muscle from human subjects. J Physiol. 2013; 591:2897–2909. [PubMed: 23529132]

Lord CC, Thomas G, Brown JM. Mammalian alpha beta hydrolase domain (ABHD) proteins: Lipid metabolizing enzymes at the interface of cell signaling and energy metabolism. Biochim Biophys Acta. 2013; 1831:792–802. [PubMed: 23328280]

Maurice DH, Palmer D, Tilley DG, Dunkerley HA, Netherton SJ, Raymond DR, Elbatarny HS, Jimmo SL. Cyclic nucleotide phosphodiesterase activity, expression, and targeting in cells of the cardiovascular system. Mol Pharmacol. 2003; 64:533–546. [PubMed: 12920188]

Morigny P, Houssier M, Mouisel E, Langin D. Adipocyte lipolysis and insulin resistance. Biochimie. 2016; 125:259–266. [PubMed: 26542285]

Oakes ND, Cooney GJ, Camilleri S, Chisholm DJ, Kraegen EW. Mechanisms of liver and muscle insulin resistance induced by chronic high-fat feeding. Diabetes. 1997; 46:1768–1774. [PubMed: 9356024]

Oka Y, Akanuma Y, Kasuga M, Kosaka K. Effect of a high glucose diet on insulin binding and insulin action in rat adipocytes. A longitudinal study. Diabetologia. 1980; 19:468–474. [PubMed: 7004966]

Perino A, Ghigo A, Ferrero E, Morello F, Santulli G, Baillie GS, Damilano F, Dunlop AJ, Pawson C, Walser R, et al. Integrating cardiac PIP3 and cAMP signaling through a PKA anchoring function of p110γ. Mol Cell. 2011; 42:84–95. [PubMed: 21474070]

Perry RJ, Camporez J-PG, Kursawe R, Titchenell PM, Zhang D, Perry CJ, Jurczak MJ, Abudukadier A, Han MS, Zhang X-M, et al. Hepatic acetyl CoA links adipose tissue inflammation to hepatic insulin resistance and type 2 diabetes. Cell. 2015; 160:745–758. [PubMed: 25662011]

Qi L, Saberi M, Zmuda E, Wang Y, Altarejos J, Zhang X, Dentin R, Hedrick S, Bandyopadhyay G, Hai T, et al. Adipocyte CREB promotes insulin resistance in obesity. Cell Metab. 2009; 9:277–286. [PubMed: 19254572]

Roberts R, Hodson L, Dennis AL, Neville MJ, Humphreys SM, Harnden KE, Micklem KJ, Frayn KN. Markers of de novo lipogenesis in adipose tissue: associations with small adipocytes and insulin sensitivity in humans. Diabetologia. 2009; 52:882–890. [PubMed: 19252892]

Rondinone CM, Carvalho E, Rahn T, Manganiello VC, Degerman E, Smith UP. Phosphorylation of PDE3B by phosphatidylinositol 3-kinase associated with the insulin receptor. J Biol Chem. 2000; 275:10093–10098. [PubMed: 10744689]

Rosen ED, Spiegelman BM. What we talk about when we talk about fat. Cell. 2014; 156:20–44. [PubMed: 24439368]

Saltiel AR, Kahn CR. Insulin signalling and the regulation of glucose and lipid metabolism. Nature. 2001; 414:799–806. [PubMed: 11742412]

Samuel VT, Shulman GI. Mechanisms for insulin resistance: common threads and missing links. Cell. 2012; 148:852–871. [PubMed: 22385956]

Savage DB, Petersen KF, Shulman GI. Disordered lipid metabolism and the pathogenesis of insulin resistance. Physiol Rev. 2007; 87:507–520. [PubMed: 17429039]

Schweiger M, Romauch M, Schreiber R, Grabner GF, Hütter S, Kotzbeck P, Benedikt P, Eichmann TO, Yamada S, Knittelfelder O, et al. Pharmacological inhibition of adipose triglyceride lipase corrects high-fat diet-induced insulin resistance and hepatosteatosis in mice. Nat Commun. 2017; 8

Sun JV, Tepperman HM, Tepperman J. A comparison of insulin binding by liver plasma membranes of rats fed a high glucose diet or a high fat diet. J Lipid Res. 1977; 18:533–539. [PubMed: 894144]

Thomas G, Betters JL, Lord CC, Brown AL, Marshall S, Ferguson D, Sawyer J, Davis MA, Melchior JT, Blume LC, et al. The serine hydrolase ABHD6 Is a critical regulator of the metabolic syndrome. Cell Rep. 2013; 5:508–520. [PubMed: 24095738]

Walenta E, Pessentheiner AR, Pelzmann HJ, Deutsch A, Goeritzer M, Kratky D, Hackl H, Oh DY, Prokesch A, Bogner-Strauss JG. α/β-hydrolase domain containing protein 15 (ABHD15)–an adipogenic protein protecting from apoptosis. PLoS One. 2013; 8:e79134. [PubMed: 24236098]

Watt MJ, Holmes AG, Pinnamaneni SK, Garnham AP, Steinberg GR, Kemp BE, Febbraio MA. Regulation of HSL serine phosphorylation in skeletal muscle and adipose tissue. Am J Physiol Endocrinol Metab. 2006; 290:E500–E508. [PubMed: 16188906]

Europe PMC Funders Author Manuscripts

Europe PMC Funders Author Manuscripts

Highlights

- ABHD15 stabilizes PDE3B, which is thereby reduced in Abhd15-deficient WAT
- ABHD15 deletion leads to unsuppressed FA release in the postprandial state
- ABHD15 ablation impairs insulin signaling
- ABHD15 contributes to the development of insulin resistance in mice and humans

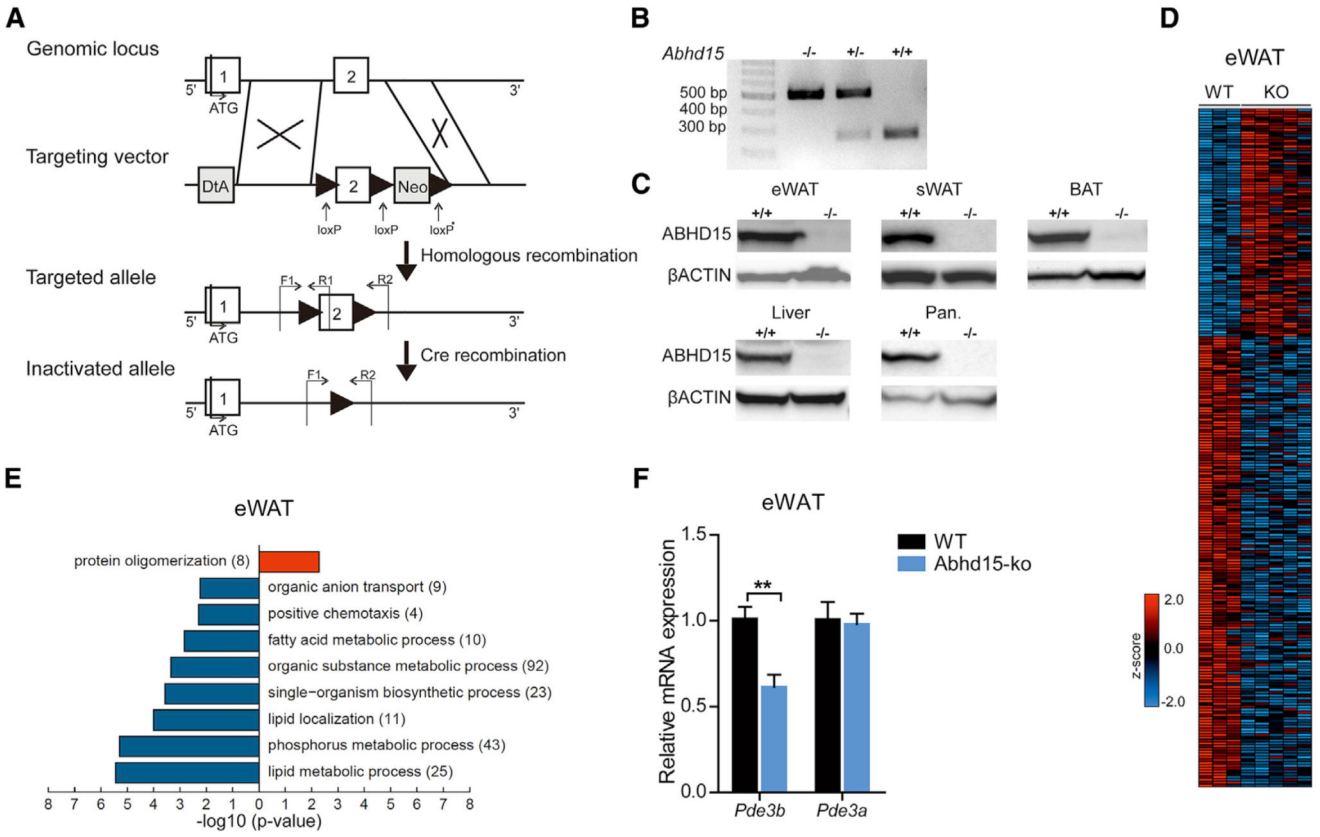

Figure 1. Generation of Abhd15-KO Mice and Microarray Analysis

(A) Schematic depiction of the generation of the knockout mouse model.

(B) Tailtip PCR of WT (+/+), heterozygous (+/−), and homozygous (−/−) Abhd15-KO mice.

(C) ABHD15 expression in tissues harvested from WT (+/+) and Abhd15-KO (−/−) mice.

(D) Heatmap of deregulated genes from microarray analyses of 1 hr-refed WT and Abhd15-KO epididymal eWAT at the age of 14 weeks on chow diet (n = 3–5).

(E) Gene ontology (GO) analysis was performed with -log10 (p value) plotted (x axis) as a function of classification meeting a p value of < 0.001. Upregulated (red) and downregulated (blue) genes in eWAT of Abhd15-KO mice are compared to controls (n = 3–5).

(F) *Pde3b* and *Pde3a* mRNA expression in eWAT (n = 6–9). Data are shown as mean ± SD. Unpaired two-tailed Student's t test was performed; statistical significance is shown as **p < 0.01. See also Figure S1 and Table S1.

Europe PMC Funders Author Manuscripts

Europe PMC Funders Author Manuscripts

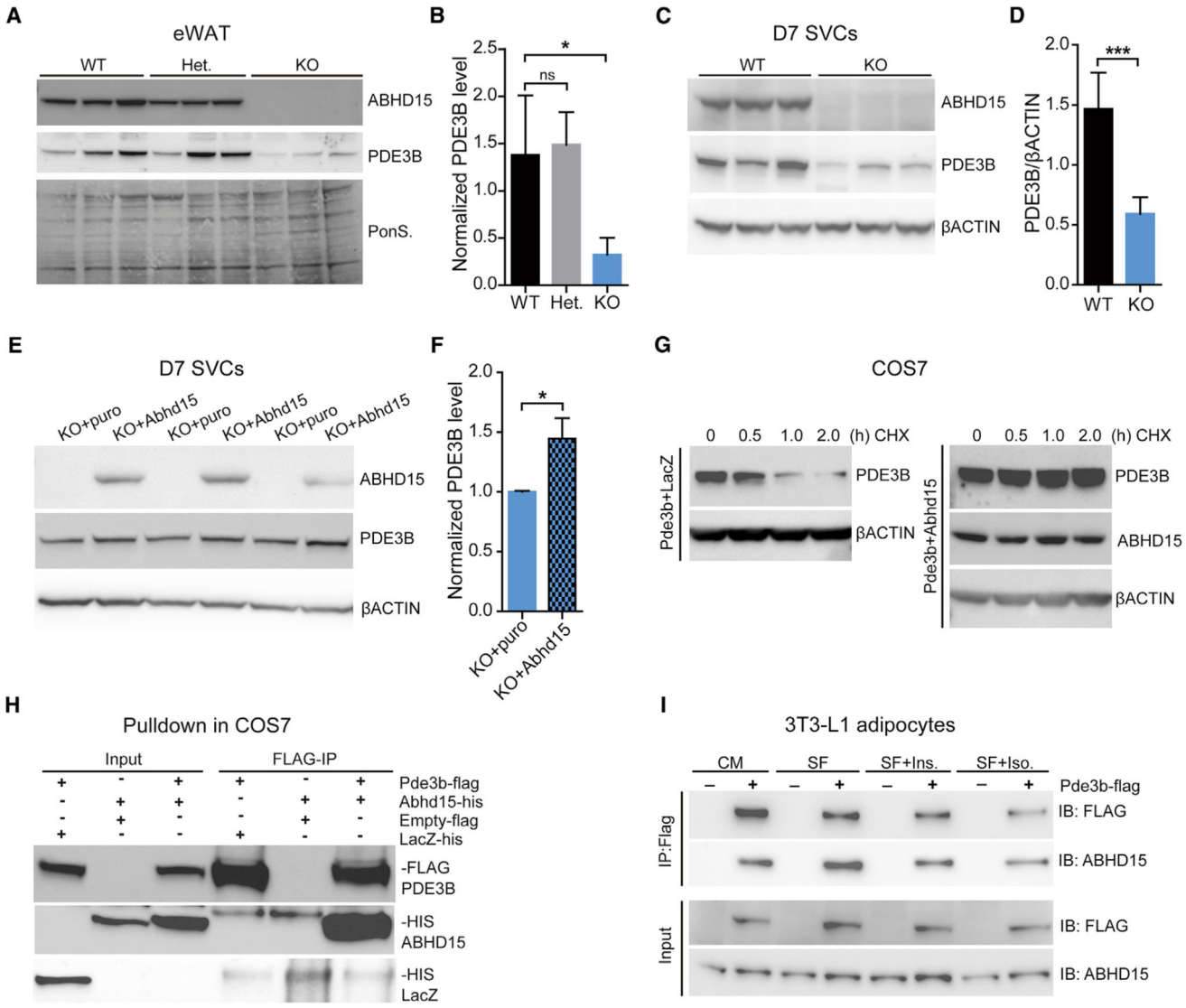

Figure 2. ABHD15 Associates with PDE3B and Regulates Its Stability and Expression

(A) Western blots (WBs) of eWAT membrane protein from WT, heterozygous (Het), and homozygous Abhd15-KO mice.

(B) Relative protein quantification of PDE3B depicted in (A) (n = 3).

(C) ABHD15 and PDE3B expression in stromal vascular cell (SVC)-derived adipocytes (n = 3).

(D) Protein quantification of PDE3B depicted in (C) and normalized to β-actin (n = 6).

(E) ABHD15 and PDE3B expression in SVC-derived Abhd15-KO adipocytes transfected with pMSCV-puro or pMSCV-Abhd15 retrovirus (n = 3).

(F) Relative protein quantification of PDE3B depicted in (E) and normalized to β-actin (n = 6).

(G) PDE3B and ABHD15 expression in COS7 cells co-transfected with Pde3b and LacZ or Pde3b and Abhd15, treated with or without 5 μg/mL cycloheximide (CHX) for the indicated time (0–2 hr).

(H) Pull-down of ABHD15 and PDE3B from co-transfected COS7 cells.
(I) Pull-down from pMSCV-puro- and pMSCV-Pde3b/FLAG-overexpressing 3T3-L1 adipocytes with M2-FLAG agarose beads. Cells were cultured in complete medium (CM), 2% FA-free BSA serum-free medium (SF) for 6 hr, then treated with 100 nM insulin and 1 μM isoproterenol for 20 min.
(B, D, and F) Data are shown as mean ± SD. Unpaired two-tailed Student's t test was performed; statistical significance is shown as *$p < 0.05$ and ***$p < 0.001$. See also Figure S2.

Europe PMC Funders Author Manuscripts

Europe PMC Funders Author Manuscripts

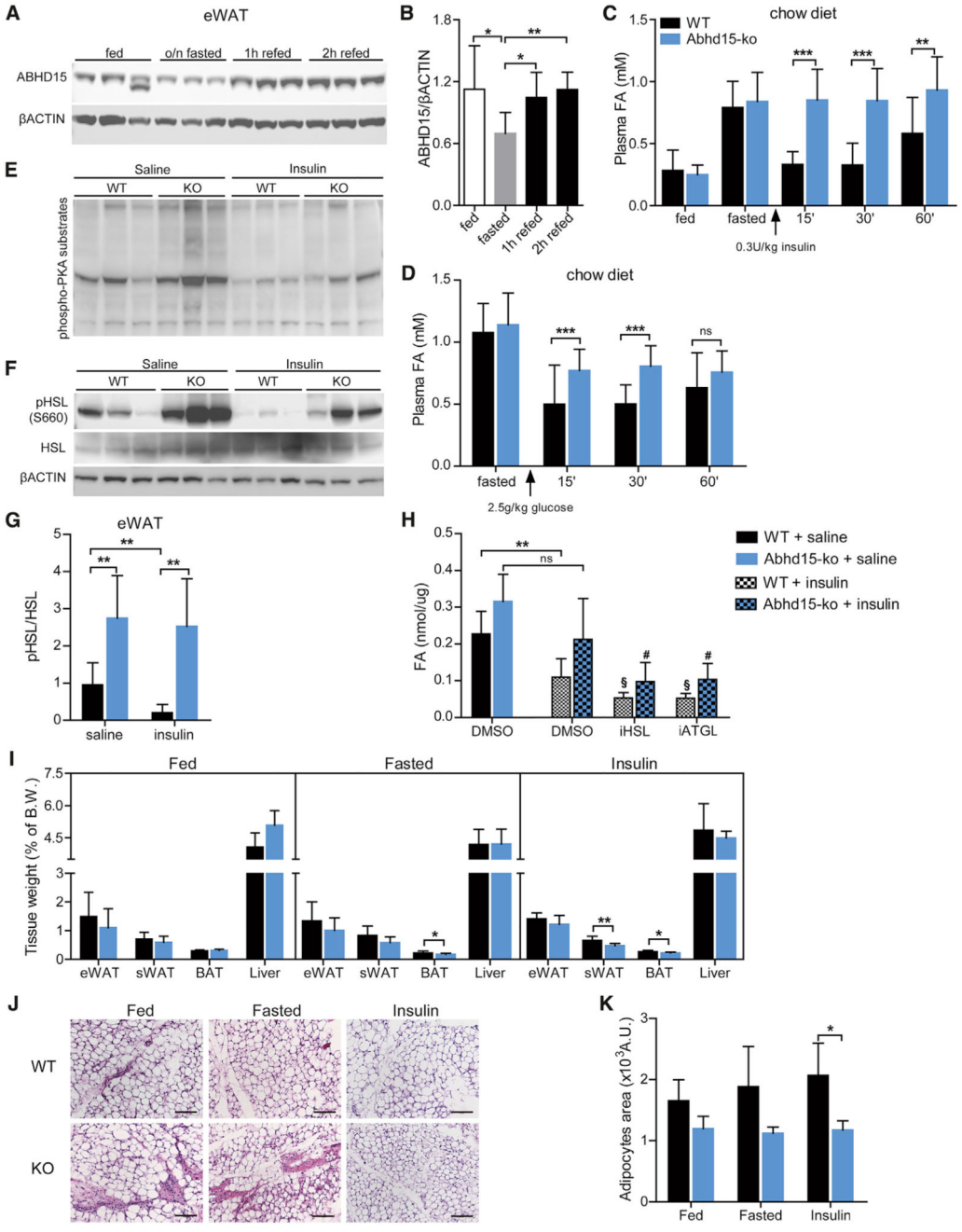

Figure 3. Abhd15-KO Mice Show Disruption of Insulin-Mediated Suppression of Lipolysis

(A) ABHD15 expression in eWAT from 12-week-old C57BL6/J mice fed chow diet *ad libitum*, overnight (o/n) fasted, or 1 hr (1h) and 2 hr (2h) refed.

(B) ABHD15 protein quantification of (A) normalized to β-actin (n = 6).

(C) 20-week-old mice were fasted overnight and then intraperitoneally (i.p.) injected with 0.3 U/kg insulin; blood was taken at the indicated time points and plasma FAs were determined (n = 6).

(D) 22-week-old mice were overnight fasted and then gavaged with 2.5 g/kg glucose. Plasma FAs were determined at the indicated time points (n = 7–8).
(E and F) Overnight-fasted 20-week-old mice were injected with saline or 0.6 U/kg insulin, and tissues were harvested 20 min later. eWAT from those mice was used for (E) PKA substrate phosphorylation and (F) HSL phosphorylation WBs (n = 3).
(G) pHSL/HSL quantification of (F) normalized to total HSL (n = 6).
(H) FA release from eWAT explants of saline- or insulin-injected (0.6 U/kg) mice. Explants were treated with 25 μM HSL inhibitor (iHSL) or 40 μM ATGL inhibitor (iATGL) for 1 hr. Symbols indicate statistical significance of insulin treatment (*), inhibitor treatment comparing WT mice (§), and inhibitor treatment comparing Abhd15-KO mice (#) (n = 4–7).
(I) 20-week-old mice on chow diet were harvested at 7 a.m. fed *ad libitum*, 12 hr fasted, or 20 min after 0.6 U/kg insulin injection. eWAT, subcutaneous (s)WAT, interscapular BAT, and liver were analyzed for their weight (n = 4–5).
(J and K) sWAT from (I) was used for (J) H&E staining, and adipocyte size was analyzed (K). Scale bar, 100 μM (n = 4–5).
(B–D, G–I, and K) Data are shown as mean ± SD. Unpaired two-tailed Student's t test was performed; statistical significance is shown as §,#,*$p < 0.05$, **$p < 0.01$, and ***$p < 0.001$. See also Figure S3 and Table S3.

Europe PMC Funders Author Manuscripts

Europe PMC Funders Author Manuscripts

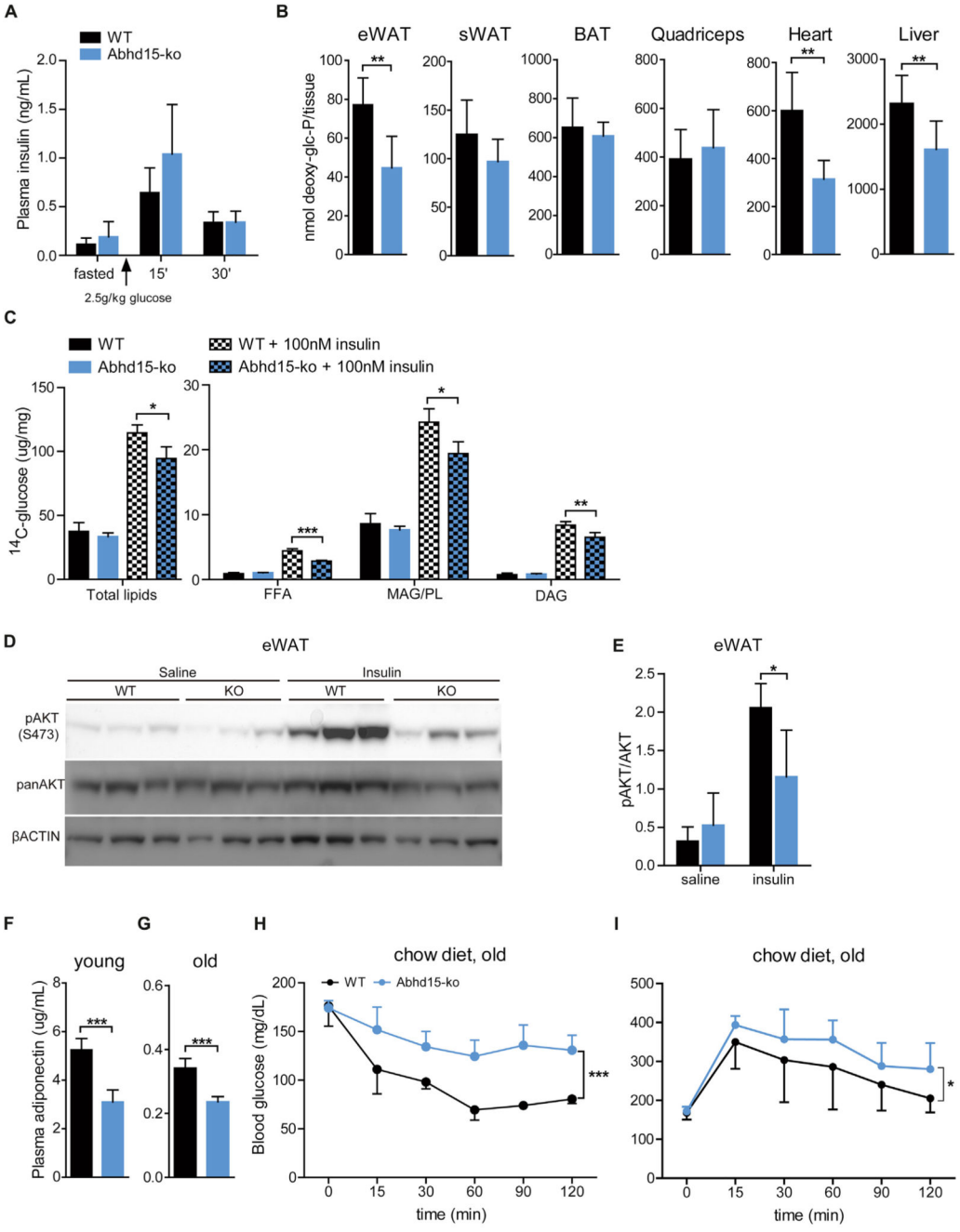

Figure 4. Abhd15-KO Mice Show Impaired Insulin-Dependent Glucose Metabolism and Develop Insulin Resistance on Chow Diet

(A) Plasma insulin levels after overnight fasting and 2.5 g/kg glucose gavage at the age of 20 weeks (n = 8).

(B) 25-week-old mice were overnight fasted and then gavaged with 2.5 g/kg glucose (spiked with 10 μCi ^{3}H-deoxyglucose per mouse). 20 min after gavage, tissues were harvested and uptake of radioactive glucose was determined (n = 7).

(C) ^{14}C-glucose incorporation into total lipids, FFA, monoacylglycerol/phospholipids (MAG/PLs), and diacylglycerol (DAG) in fully differentiated SVCs (n = 4).

(D) pAKT and panAKT expression in eWAT harvested from overnight-fasted 20-week-old mice after saline or insulin injection (as in Figures 3E and 3F).
(E) Protein quantification of (D) normalized to panAKT (n = 6).
(F and G) Plasma adiponectin levels were measured after overnight fasting and then 1-hr refeeding at the age of (F) 20 weeks (young) and (G) 54 weeks (old).
(H) 60-week-old mice were fasted for 4 hr, then injected with 0.35 U/kg insulin, and glucose levels were measured at the indicated time points (n = 6).
(I) 80-week-old mice were fasted for 6 hr, then injected with 2.5 g/kg glucose, and glucose levels were measured at the indicated time points (n = 4).
(A–C and E–I) Data are shown as mean ± SD. Unpaired two-tailed Student's t test or two-way ANOVA (multiple datasets) was performed; statistical significance is shown as *p < 0.05, **p < 0.01, and ***p < 0.001. See also Figure S4.

Europe PMC Funders Author Manuscripts

Europe PMC Funders Author Manuscripts

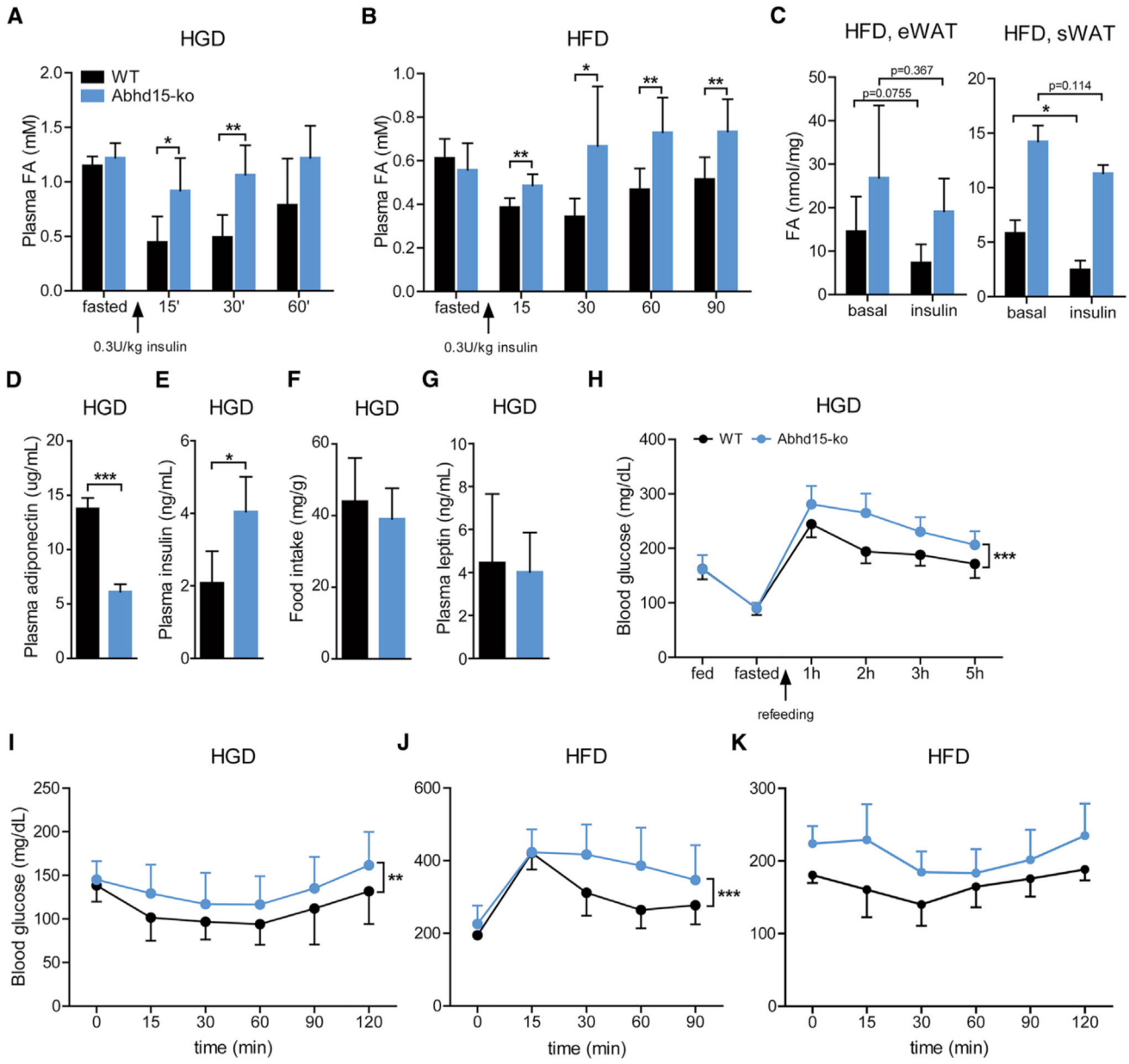

Figure 5. Abhd15-KO Mice Develop Insulin Resistance on High-Glucose and High-Fat Diets

(A) 8-week-old mice on high-glucose diet (HGD) for 12 weeks. Thereafter, mice were overnight fasted and injected with 0.3 U/kg insulin, and plasma FA levels were determined (n = 5–6).

(B) 10-week-old mice on high-fat diet (HFD) for 12 weeks. Thereafter, mice were overnight fasted and injected with 0.35 U/kg insulin, and plasma FA levels were determined (n = 8).

(C) FA release from explants of eWAT and sWAT of mice on HFD with or without 100 nM insulin treatment (n = 4).

(D and E) Plasma adiponectin (D) and insulin (E) levels were measured in HGD-fed mice at the age of 25 weeks, fasted overnight, and then refed for 2 hr (n = 4).

(F) Food intake was measured in HGD-fed mice at the age of 25 weeks, fasted overnight, and then refed for 5 hr (n = 5–7).
(G) Plasma leptin levels were measured in HGD-fed mice at the age of 25 weeks, fasted overnight, and then refed for 2 hr (n = 4).
(H) Blood glucose levels were measured in HGD-fed mice at the age of 25 weeks from tail vein blood at the indicated states and time points (n = 7–8).
(I) 8-week-old mice on HGD for 44 weeks. Thereafter, mice were fasted for 4 hr and injected with 0.25 U/kg insulin, and glucose was determined at the indicated time points (n = 7).
(J) 8-week-old mice on HFD for 32 weeks. Thereafter, mice were fasted for 6 hr and injected with 1 g/kg glucose, and glucose was determined at the indicated time points (n = 7).
(K) 8-week-old mice on HFD for 30 weeks. Thereafter, mice were fasted for 4 hr and injected with 0.5 U/kg insulin, and glucose was determined at the indicated time points (n = 7).
(A–K) Data are shown as mean ± SD. Unpaired two-tailed Student's t test or two-way ANOVA (multiple datasets) was performed; statistical significance is shown as *$p < 0.05$, **$p < 0.01$, and ***$p < 0.001$. See also Figure S4.

Europe PMC Funders Author Manuscripts

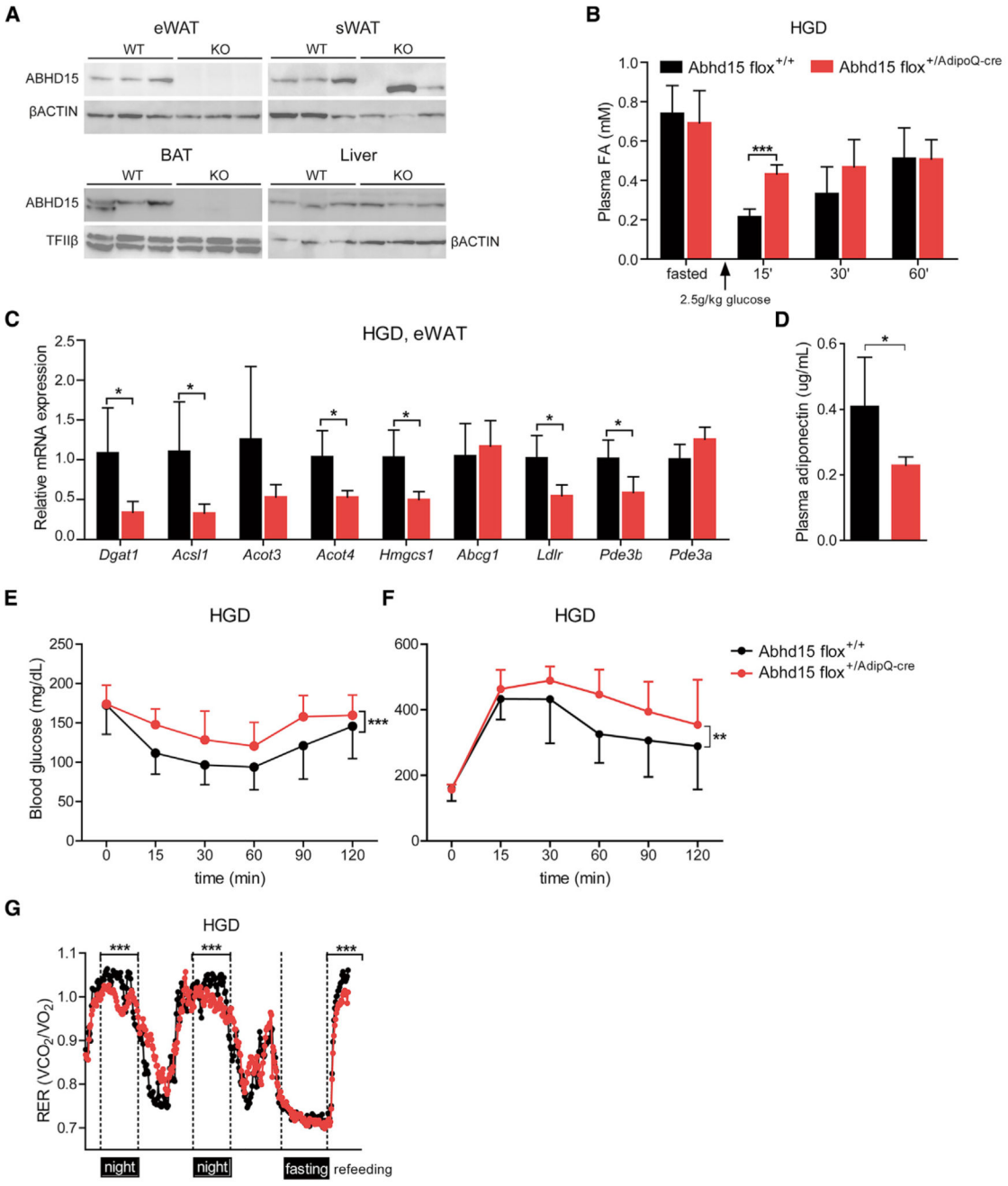

Figure 6. Adipose Tissue-Specific Ablation of ABHD15 Is Responsible for the Phenotype Observed in Global Abhd15-KO Mice

(A) ABHD15 expression in tissues harvested from WT (Abhd15 flox$^{+/+}$) and KO (Abhd15 flox$^{+/AdipoQ\text{-}cre}$) mice.

(B) 20-week-old Abhd15 flox$^{+/+}$ and Abhd15 flox$^{+/AdipoQ\text{-}cre}$ on chow diet were fasted overnight and gavaged with 2.5 g/kg glucose. Facial vein blood was drawn at the indicated time points and FA levels were measured (n = 6–8).

(C) Relative mRNA expression of lipid metabolism and *Pde3* genes in eWAT on HGD in the 1-hr-refed state (n = 3–5).

(D) Plasma adiponectin levels of mice on HGD was measured after overnight fasting and then 1-hr refeeding (n = 3–5).
(E) 8-week-old mice on HGD for 32 weeks. Thereafter, mice were fasted for 4 hr and injected with 0.25 U/kg insulin, and glucose was determined at the indicated time points (n = 7–8).
(F) 8-week-old mice on HGD for 33 weeks. Thereafter, mice were fasted for 6 hr and injected with 2.5 g/kg glucose, and glucose was determined at the indicated time points (n = 7–8).
(G) Respiratory exchanged ratio (VCO_2/VO_2) was measured in 30-week-old mice on HGD over 3 days including overnight fasting and 6-hr-refeeding period (n = 3–5).
(B–G) Data are shown as mean ± SD. Unpaired two-tailed Student's t test or two-way ANOVA (multiple datasets) was performed; statistical significance is shown as *$p < 0.05$, **$p < 0.01$, and ***$p < 0.001$. See also Figure S5.

Europe PMC Funders Author Manuscripts

Europe PMC Funders Author Manuscripts

Table 1

Correlations of *ABHD15* Gene Expression in OWAT from Severely (BMI > 40 kg/m^2) Obese Patients and Several Metabolic Parameters

Insulin Sensitivity			Insulin Resistance			Other Parameters		
Parameter	**Spearman's rho**	**p**	**Parameter**	**Spearman's rho**	**p**	**Parameter**	**Spearman's rho**	**p**
OGIS	0.66	0.02	first phase response	−0.62	0.04	IL-6	−0.70	0.02
ISI	0.68	0.03	second phase response	−0.62	0.03	FFA	−0.69	0.02
CLIX	0.64	0.03	AUC OGTT	−0.65	0.02			
			HOMA-IR	−0.53	0.07			